

LATTICE DESIGN OF 250 MeV VERSION OF PERLE

A. Fomin*, L. Perrot, J. Michaud, R. Abukesh, C. Guyot
 Universite Paris-Saclay, CNRS/IN2P3, IJCLab, Orsay, France
 S. A. Bogacz[†], Jefferson Lab, CASA, Newport News, USA

Abstract

The PERLE (Powerful Energy Recovery LINAC for Experiment) collaboration is working on a high power energy recuperation linac facility with three acceleration (up to 500 MeV) and three deceleration passes through two cryo-modules with an injection current of 20 mA. Here we present the lattice design of the first phase of this machine, which features a single cryo-module and demonstrates six-pass operation at a maximum energy of 250 MeV at a high current. This initial lattice design boasts a simpler structure with fewer elements, resulting in lower initial costs, faster construction and shorter commissioning time. Furthermore, all magnets and cryo-modules are designed to be compatible with both phases, keeping upgrade costs to a minimum.

OBJECTIVES OF 250 MeV VERSION

The PERLE (Powerful Energy Recovery Linac Experiment) [1] machine is aimed at demonstrating six-pass operation of the ERL (Energy Recovery Linac) at a high current of 20 mA and the energy of up to 500 MeV. The lattice of the full power machine [2,3] consists of two Common Sections with linacs connected to six Arcs by two Spreaders and two Recombiners (see Fig. 1).

In fact, with minimal additional costs in hardware, it is feasible to split the construction of this machine into two

phases: “250 MeV” version with one cryo-module (containing four RF-cavities) and three Straight Sections at opposite sides, and “500 MeV” version with two cryo-modlues at opposite sides (see Fig. 1). This approach not only allows for a more manageable and efficient build, but also provides the opportunity to thoroughly test and optimize each section. This can lead to a more streamlined and cost-effective overall process, as any issues or improvements can be identified and addressed before moving the full power machine.

Of course, it should be noted that upgrading to the 500 MeV version will require additional expenses, manpower, and shutdown time for reassembly and recommissioning. Therefore, careful planning and consideration should be given to the decision to upgrade and the overall cost-benefit analysis of the project.

All of the magnets and the cryo-module are chosen to be compatible with both versions, thus in terms of hardware for the first phase we would need to add just about 30 meters of beam pipes and the power supplies with less current for some of the magnets.

The fundamental difference of 250 MeV version is that the injection line and the dump are on the same side. This leads to a slightly longer overall footprint (28.6→29.9 m) as the corrector magnets for the injection and dump should be located before and after the cryo-module (see Fig. 1).

Another benefit of 250 MeV version is that the place for the experimental area is larger, so it is possible to have two or even more low-beta experimental areas with easier access.

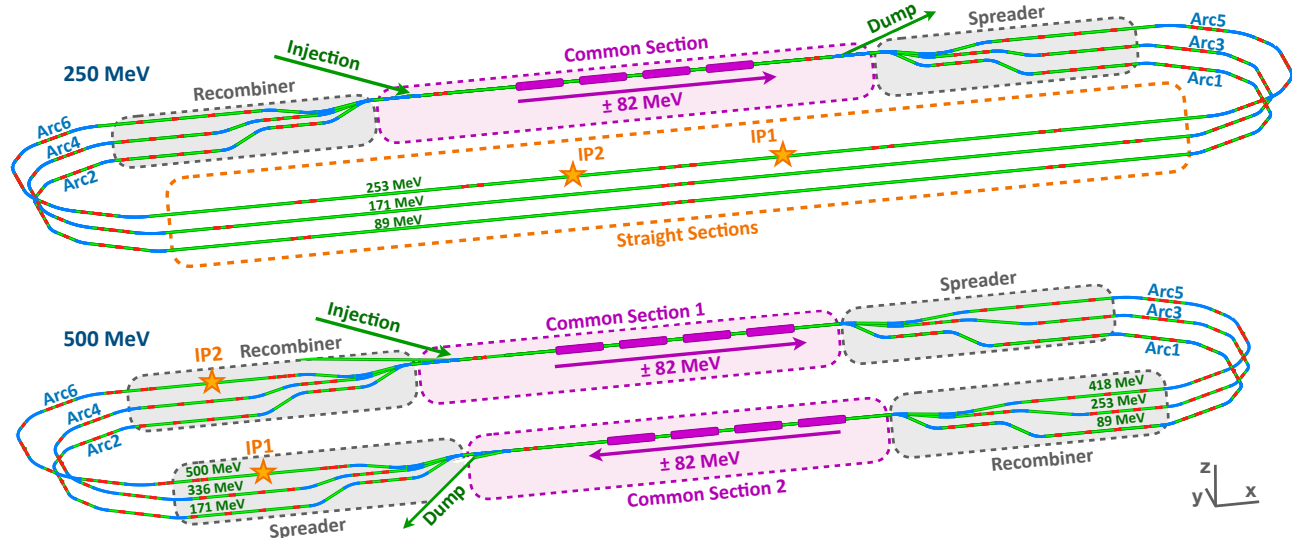


Figure 1: Baseline layout of 250 MeV (top) and 500 MeV (bottom) versions of PERLE: pipe lines (green), dipole (blue) and quadrupole (red) magnets, RF cavities (purple), experimental areas with low beta (orange).

LATTICE DESIGN

The main objective in designing the 250 MeV version is to utilize the same elements and section designs as the nominal power machine wherever possible, in order to minimize both the cost and time required for the upgrade. To maintain consistency between the two versions, the Arcs share the same design and the Spreader and Recombiner of the 250 MeV version feature a design similar to that of the 500 MeV version near Arcs 2, 4, and 6.

To reduce initial costs, construction time and commissioning time, the layout of the 250 MeV version features three Straight Sections replacing the Recombiner, the second Common Section, and the second Spreader (see Fig. 1).

Both versions of ERL utilize a racetrack topology in which the turn sections, tuned for a specific energy, are shared by both the accelerating and decelerating beams. Therefore, for the accelerating and decelerating linac passes of the same energy, it is necessary for the TWISS function to be identical, and the TWISS function of the turn sections should be symmetrical.

Common Section

The first part of the 250 MeV version's Common Section, spanning from the Chicane magnets up to the end of the Cryo-Module, is identical to that of the 500 MeV version. However, immediately after the Cryo-Module, a mirrored Injection compensation array of magnets for the Dump is added (as shown in Fig. 2). This addition makes the Common Section of the 250 MeV version two meters longer than that of the 500 MeV version.

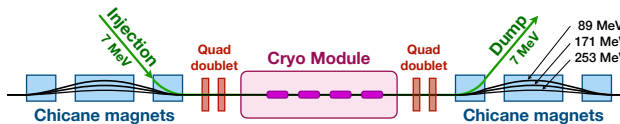


Figure 2: Common Section layout of 250 MeV version.

A pseudo-periodic solution was obtained for the TWISS function in the Common Section of the 250 MeV version of PERLE by using MAD-X [4] calculations, supplemented by analytical model of the transverse focusing of the RF cavity by J.B. Rosenzweig and L. Serafini [5]. The solution was verified in [6] by comparing it to tracking results obtained with ASTRA [7]. This solution was found for the three accelerating and three decelerating passes (as shown in Fig. 3).

The plot shows that the beta function takes a parabolic shape with a maximum value of approximately 12 meters at the highest energy passes, but becomes asymmetric at lower energies due to transverse focusing and has smaller initial betas. Quadrupole doublets can be used to further correct the beam size at the Injection and Dump chicane magnets, this is outside the scope of this study. Furthermore, the final values of TWISS parameters after each pass serve as the starting TWISS parameters for the Turn Sections' optics calculations.

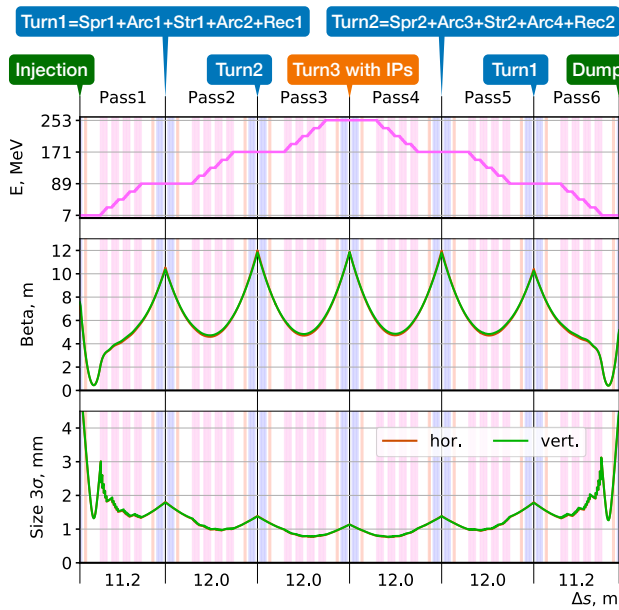


Figure 3: Beam energy, beta function and size during six passes through the Common Section.

Turn Sections

The Turn Sections of the 500 MeV version consist of Spreader-Arc-Recombiner Sections, which turn the beam by 180 degrees and direct it to the other Common Section with the same beta function. On the other hand, the Turn Sections of the 250 MeV version comprise Spreader-Arc-Straight-Arc-Recombiner Sections, which turn the beam by 360 degrees and direct it back to the beginning of the same Common Section. Figure 4 shows the layout of the Spreader Section, and the Recombiner Section mirrors its design.

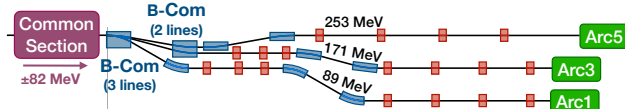


Figure 4: Spreader Section layout.

Each Turn Section is symmetrized together with Arcs and Straight sections that it contains and beam size of 3σ is kept under 2.2 mm (see Fig. 5). The Turn Section of middle energy is not sticky symmetrized as Arc3 and Arc4 have different dipole lengths, but the initial and final TWISS function are symmetric. Arcs have an identical design to 500 MeV version with the same magnets retuned for the lower energies and to get no horizontal dispersion and momentum compaction M56 in the straight sections. The Straight Section with the top energy in this design is at the top for the easier access to the two IPs with $\beta < 30$ cm.

In the 250 MeV version, the number of dipole magnets is reduced to a total of 60, representing a reduction of 18 magnets from the nominal power machine design. Similarly, the number of quadrupole magnets can be reduced by 11 to a total of 131, with the field gradient kept under

22 T/m. This contrasts with the 500 MeV version, in which 9 quadrupoles have gradients over 38 T/m, which exceeds the current magnet design's saturation threshold [8].

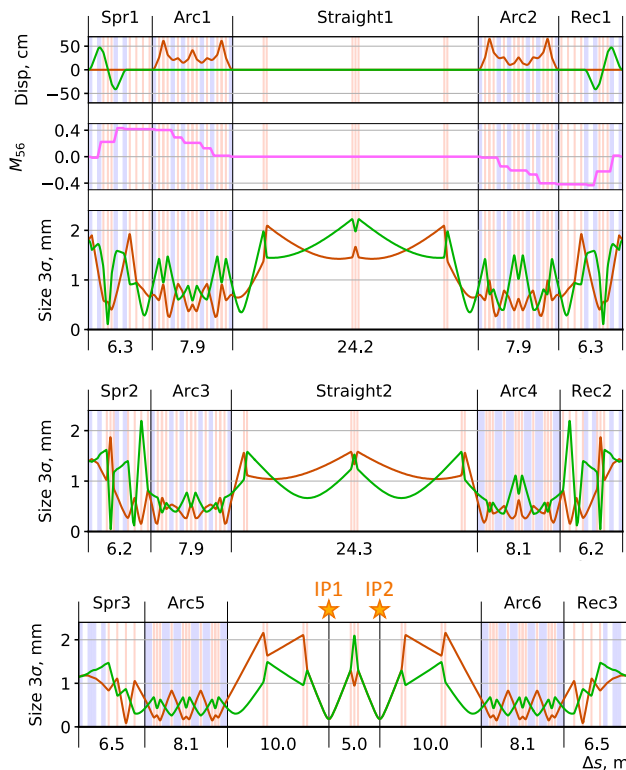


Figure 5: Beam dispersion, compaction factor and size during Turn1 and beam size during Turn2 and Turn3. Red and green curves for parameters in horizontal and vertical planes, respectively.

CONCLUSION

In summary, building the PERLE machine in two phases offers a viable solution for reducing the construction and commissioning time needed to demonstrate six passes ERL

operation at half of the nominal power. Although the upgrade to the second phase will require additional expenses, manpower, and shutdown time, the phased approach provides ample opportunities to optimize and test each section of the machine before moving to the final version. Moreover, the two-phased construction can be accomplished with a similar footprint and without significant additional costs in hardware. Overall, the proposed approach offers a promising path forward for building a more efficient and cost-effective high-power energy recuperation linac facility.

REFERENCES

- [1] D. Angal-Kalinin *et al.*, "PERLE. Powerful energy recovery linac for experiments. Conceptual design report", *J. Phys. G: Nucl. Part. Phys.*, vol. 45, no. 6, p. 065003, May 2018. doi:10.1088/1361-6471/aaa171
- [2] S. A. Bogacz *et al.*, "PERLE - Lattice Design and Beam Dynamics Studies", in *Proc. IPAC2018*, Vancouver, BC, Canada, May 2018. doi:10.18429/JACoW-IPAC2018-THPMK105
- [3] S. A. Bogacz, "Lattice Design (Including IR)", presented at PERLE Collaboration Meeting, Orsay, France, Jan. 2022. https://indico.ijclab.in2p3.fr/event/7907/contributions/24618/attachments/18115/23953/PERLE_Collab_2022.ppt
- [4] <http://madx.web.cern.ch/madx/>.
- [5] J. B. Rosenzweig and L. Serafini. "Transverse particle motion in radio-frequency linear accelerators", *Phys. Rev. E*, vol. 49, pp. 1599–1602, 1994. doi:10.1103/PhysRevE.49.1599
- [6] C. Guyot *et al.*, "Modeling of Standing Wave RF Cavities for Tracking through Multi-Pass Energy Recovery Linac", presented at IPAC'23, Venice, Italy, May 2023, paper TUPL170, this conference.
- [7] K. Floettmann, ASTRA: A space charge tracking algorithm documentation, <http://www.desy.de/~mpyflo/>.
- [8] R. Abukeshk *et al.*, "Magnetic Design of the Commutational Magnet and Quadrupoles for PERLE Accelerator" presented at IPAC'23, Venice, Italy, May 2023, paper MOPA023, this conference.